# Modelica Component Models for Non-diffracting Floating Objects and Quasi-static Catenary Moorings

Savin Viswanathan[1] Christian Holden[1]

[1]Dept. of Mechanical and Industrial Engineering, Norwegian University of Science and Technology (NTNU), NO-7491 Trondheim, Norway. {savin.viswanathan,christian.holden}@ntnu.no

## Abstract

In this paper, the theory behind determining the hydrodynamic response of a floating object in the presence of waves is discussed, followed by a simplification for the case of wave-transparent objects. The Morison equation is introduced as a means to estimate lateral wave and current loads on slender bodies. The quasi-static catenary approach to determine mooring forces is then discussed. Development of *Modelica* component-models to simulate the hydrodynamic response of free-floating and catenary-moored non-diffracting objects, in the presence of waves and depth varying current, is then dealt with in detail, and the results dicussed.

*Keywords: hydrodynamics of non-diffracting floating objects, quasi-static catenary mooring, Modelica ocean-engineering library.*

## 1 Introduction

The advantages of developing an *OpenModelica* ocean-engineering library populated with domain-specific *component-models* and *functions* to carry out the integrated simulation of multi-pyhsical ocean engineering systems was demonstrated by the authors (Viswanathan and Holden, 2019). This earlier work:

1. Gives a brief description of the simulation of systems based on the hydrodynamic response of catenary-moored non-diffracting floating objects in the presence of waves and current,

2. Demonstrates the satisfactory agreement of the *Modelica* simulation results with those obtained using a popular ocean-engineering commercial software (*Orcaflex*), and

3. Brings out the advantages of using a component-model based simulation approach.

The voluminous nature of the earlier work precluded the possibility of delving into the theoretical and implementational details of the various *Modelica* component-models of the ocean-engineering library proposed by the authors, the preliminary version of which is available for download at `github.com/Savin-Viswanathan/OELib_OMAE2019`.

(Viswanathan and Holden, 2020) gives a detailed description of the development of *Modelica* component-models to simulate regular as well as irregular waves and depth-varying current. This present work elaborates on the theoretical and implementational details of the component-models for non-diffracting floating objects, and catenary mooring based on the quasi-static approach.

## 2 Theory

### 2.1 Hydrodynamics

Considering the steady-state interaction of a floating object with a regular wave, the loads acting on the body may be considered to be comprised of:

- The fluid pressure loads due to the *incident* wave acting on the body, which is assumed fixed at its mean position.

- The fluid pressure loads due to the *scattered/diffracted* wave from the body, which is assumed fixed at its mean position.

- The fluid pressure loads due to the *radiated* wave system set up by the body as it oscillates in its six Degrees-of-Freedom (DoF) in calm water.

An illustration of the *Diffraction-Radiation* problem is given in Figure 1.

The loads due to the incident wave are referred to as *Froude-Krylov* loads, and those due to the scattered wave are referred to as *diffraction* loads in p. 39 of (Faltinsen, 1999), and this is the convention followed in this work. Another widely used convention is to refer to the combined incident and scattered wave-problem as the *diffraction* problem as in p. 288 of (Newman, 1989).

The Froude-Krylov and diffraction loads taken together constitute the wave excitation loads and may be determined by integrating the incident and diffracted wave dynamic pressures over the mean wetted hull surface. The integration of the dynamic component of the radiation wave pressures give the associated hydrodynamic loads commonly referred to as *added-mass* and *damping*, while the integration of the hydrostatic component gives the *restoring* loads. The added-mass loads are in phase with the body acceleration and the damping loads are in phase with the body velocity.

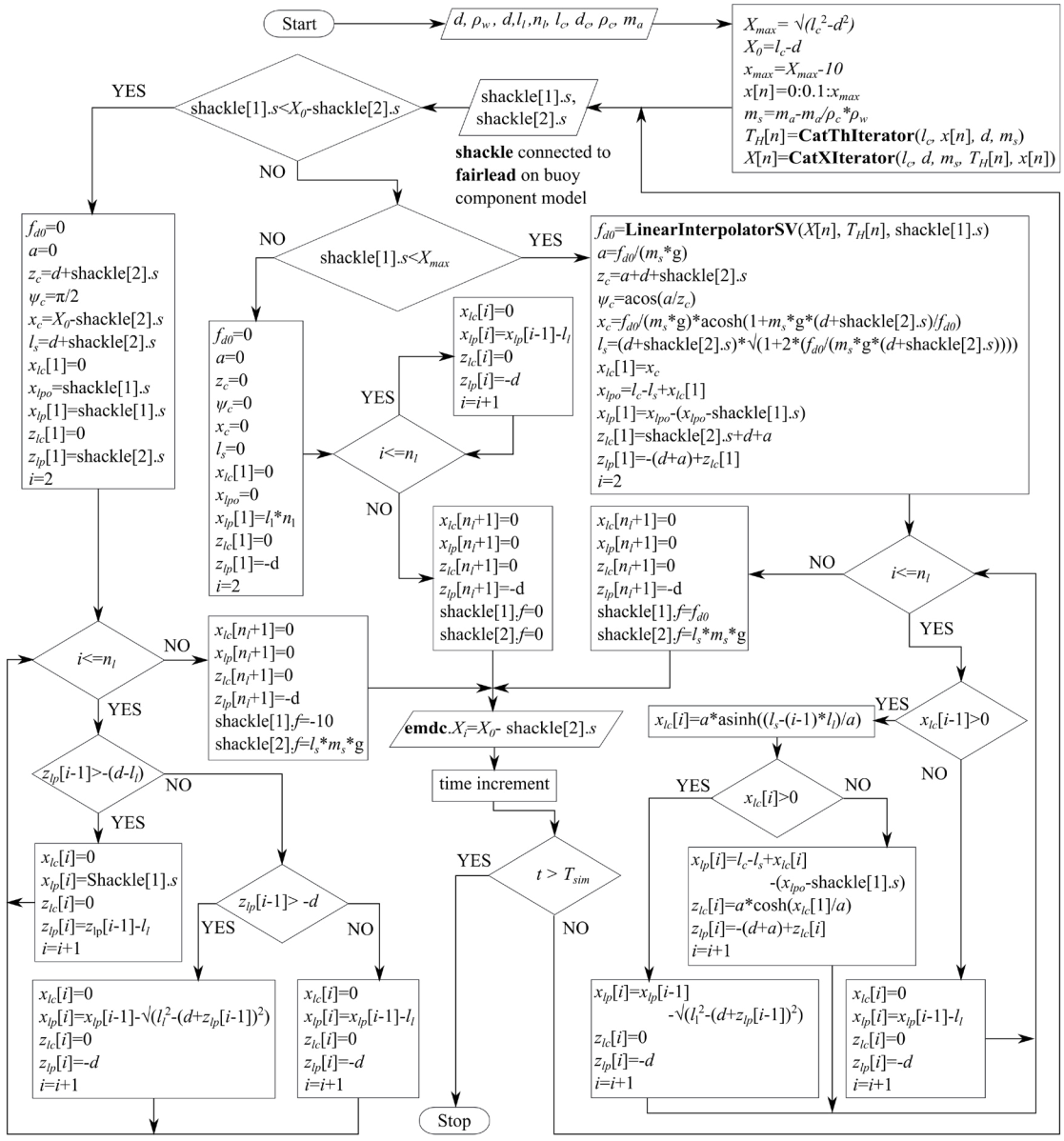


**Figure 4.** Flow-chart for the quasi-static catenary component-model.

A composite connector **Shackle[2]**, having two flanges of type *Modelica.Mechanics.Translational.Interfaces.Flange_b*, is specified at the top end of the catenary to transfer the horizontal and vertical mooring loads. The parameters defined are the water depth $d$ [m], water density $\rho_w$ [kg/m$^3$], the number of segments into which the mooring is discretized $n_l$, the length of each segment $l_l$ [m], the density of the mooring material $\rho_c$ [kg/m$^3$], and the dry specific mass of the chain $m_a$ [kg/m]. Since the **Shackle** is connected to the **Fairlead**, the corresponding positional data are also available.

$X_{max}$, $X_0$, $x_{max}$ [m] are calculated along with the submerged specific mass of the mooring $m_s$ [kg/m]. The vector containing the $x$ positions, where the horizontal mooring load is to be iterated, is defined as $x[n]$. A *function* **CatThIterator** returns the vector $T_H[n]$, containing the corresponding horizontal tension values, calculated based on (14). Another *function* **CatXIterator**, returns the vector $X[n]$ containing the $X$ position corresponding to the $x$ position, as defined in Figure 2.

A data connector **emdc** is specified to link the wave and current data from the **EnvironmentBus** to the mooring. In addition, the initial $x$ co-ordinate of the top end of the mooring line $X_i$ [m], is transmitted to the universal data bus for utilization by the buoy component-model to specify its initial condition.

$f_{d0}$ [N] is the horizontal mooring load, for the given $x$

co-ordinate of the top end of the mooring line, $a$ is the catenary parameter, $z_c$ [m] is the $z$ co-ordinate of the top end of the catenary, in the local co-ordinate system of the catenary, the origin of which lies at a distance of $a$ [m] below the bottom-most point of the catenary, as described in (Tatum, 2004). $\psi_c$ [rad] is the slope of the top-most catenary segment, $x_c$ [m] is the $x$ co-ordinate of the top-most point of the catenary, and $l_s$ [m] is the suspended length of the catenary.

$x_{lc}$ and $z_{lc}$ are vectors holding the $x$ and $z$ co-ordinates of the end points of the segments, in the local co-ordinate system of the catenary. $x_{lp}$ and $z_{lp}$ are the vectors holding the $x$ and $z$ co-ordinates of the end points of the segments, in the global coordinate system. $x_{lpo}$ is the plot correction parameter to account for the minor difference between the actual catenary shape with its top end $z$ coordinate corresponding to the instantaneous position of the buoy keel, and the catenary shape which is back-calculated based on the horizontal tension value from the look-up table, which is in turn based on the $z$ co-ordinate of the top end of the catenary lying at the sea-surface.

If the $x$ co-ordinate of the shackle is less than $X_{min}$ [m], then a small force in the positive $x$ direction is applied to restore the buoy to a region where the mooring model is valid. The vertical mooring load is then the weight of the vertically suspended length of the mooring. For the rare cases when shackle[1].$s < X_{min}$, the plot of the mooring shows a vertically suspended-length instead of the actual shape.

When the $x$ co-ordinate of the shackle is between $X_{min}$ and $X_{max}$, the horizontal mooring load is the corresponding value interpolated from the lookup-table using a *function* **linearInterpolatorSV**, and the vertical load is based on the suspended length back-calculated from the horizontal load. The plot of the mooring line shows the catenary shape, back-calculated from the horizontal load, and corrected using $x_{lpo}$.

If the loads on the buoy exceed the capacity of the mooring line, then the $x$ co-ordinate of the shackle exceeds $X_{max}$, the catenary is assumed to be detached from the buoy, and would lie extended on the sea-floor.

### 3.2.1 Current and Wave Loads on the Mooring Line

Simulation of current and wave Morision loads on the mooring line is based on the theory given in Section 2.2. The methodology is similar to the one represented by Figure 4, with additional loops for determining fluid and structure velocities and accelerations, and is easily discernible from the code. **Catenary_Mooring_MfC** considers the Morison loads due to current and mooring velocities, while **Catenary_Mooring_MfCW** considers the loads due to current, wave, and mooring line velocities and accelerations.

## 4 Results

The simulation files for all results discussed below are available at `github.com/Savin-Viswanathan/Modelica2020-b`. Comparison results using *Orcaflex* are also presented here.

Figure 5a shows the heave response of a cylindrical buoy of $r = 0.6$ [m], $h = 2$ [m], $m_s = 350$ [kg], $m_b = 500$ [kg], in a water depth of $d = 50$ [m], when subjected to a regular wave with $H_r = 1$ [m] and $T_r = 7$ [s], with $T_{del} = 0$ [s], and $T_{rmp} = 20$ [s]. We have assumed $C^x_{ma} = C^z_{ma} = 1$, $C^x = 0$ [kg/s], and $C^z = 3100$ [kg/s].

Figure (4) in (Viswanathan and Holden, 2019) had shown the same results for heave, and we had noticed a slight discrepancy between the *Modelica* and *Orcaflex* results. The cause was identified to be an error in the treatment of the added mass term in (4) of (Viswanathan and Holden, 2019), and has been corrected based on the theory described here in Section 2.1.1.1. Figure 5b shows the surge response.

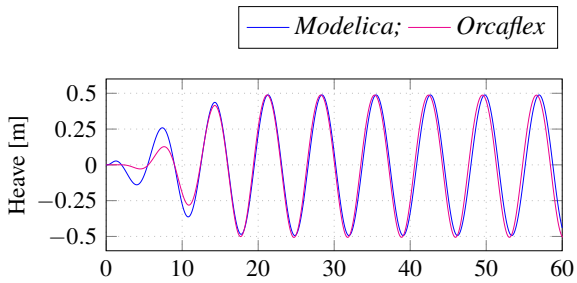


**(a)** Heave response.

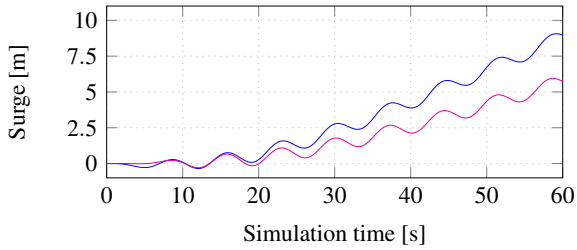


**(b)** Surge response.

**Figure 5.** Unmoored cylindrical buoy in waves.

Figure 6a shows the surge response of the above buoy, in the presence of a uniform current of 1 [m/s] in the $x$ direction, while Figure 6b shows the same in presence of both the above wave and current.

Figure 7a shows the horizontal Morison loads on a fixed buoy with same properties as the earlier one, but with a draught of 1 [m], when subjected to a uniform current of 1 [m/s]. Figure 7b shows the surge Morison loads when only a regular wave, with the same parameters as above, acts on the fixed buoy, and Figure 7c shows the Morison loads when both the current and the wave acts on the buoy.

From Figure 7, we observe that the Morison loads are a close match, and hence, the difference between *Modelica* and *Orcaflex* values in Figures 5b, 6a, and 6b, can be attributed to the difference in the way in which the loads are ramped up during the start of simulation, as evid-

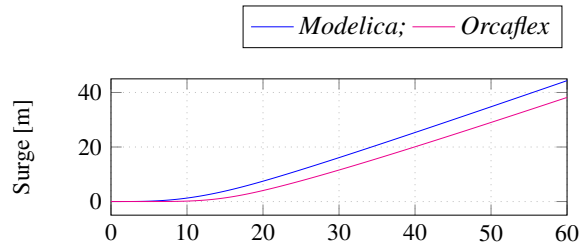


**(a)** Current only.

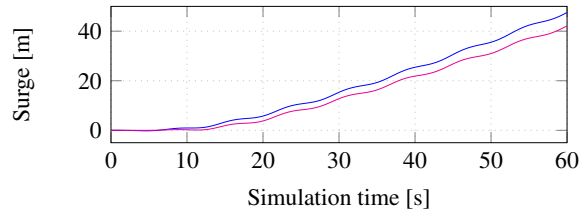


**(b)** Wave and current.

**Figure 6.** Surge response of an unmoored cylindrical buoy.

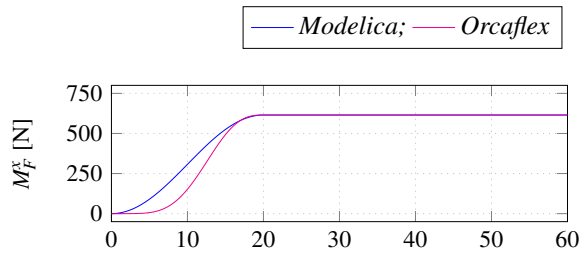


**(a)** Current only.

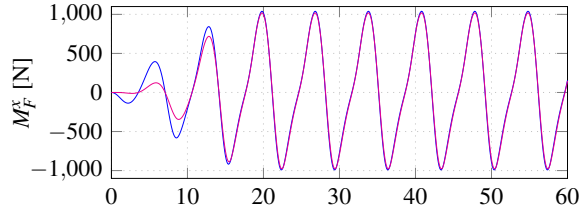


**(b)** Wave only.

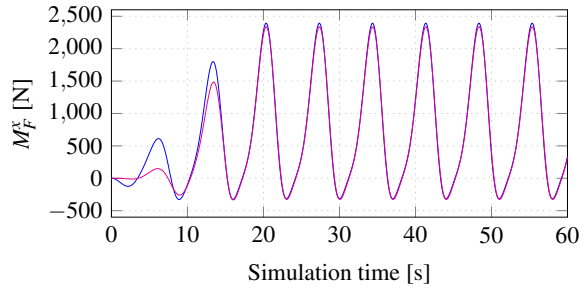


**(c)** Waves and current.

**Figure 7.** Morison loads on a fixed cylinder.

ent from Figure 7a. *Orcaflex* uses *vertical-stretching* of the water-particle kinematics, while the present *Modelica* model employs *moved* kinematic-profiles, and this could be the cause of the minute difference in peak values of the Morison loads in Figures 7b and 7c.

*Orcaflex* uses a lumped-mass and spring-damper model for the mooring lines, while mooring forces in the present work are based on the quasi-static catenary theory. Figure 8 shows the horizontal tension values given by *Orcaflex* and *Modelica* models for different $X$ positions, for moorings of different specific masses. The horizontal tensions are a close fit, with *Modelica* giving slightly higher values than *Orcaflex*. e.g., for a chain with specific mass of 16 [kg/m], at $X = 70$ [m], $T_H$ in *Modelica* is 2,336 [N] and 2,299 [N] in *Orcaflex*. The mooring horizontal tensions from *Orcaflex* were determined by placing the top end of the line at different $X$ positions along the free surface manually and a small error in the values had occured in Figure 10 of (Viswanathan and Holden, 2019).

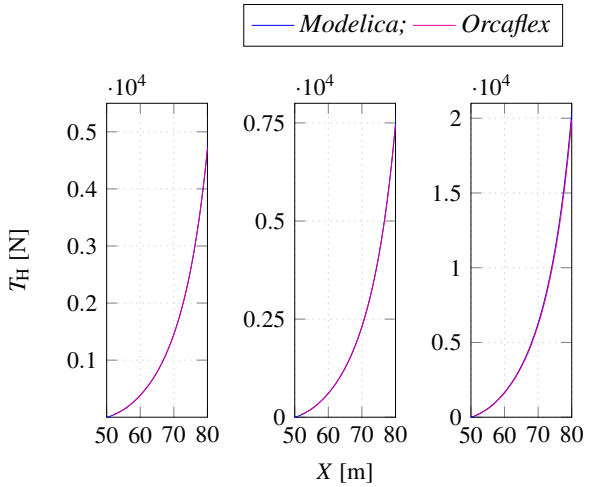


**(a)** $m_a = 10$ kg/m **(b)** $m_a = 16$ kg/m **(c)** $m_a = 43.5$ kg/m

**Figure 8.** Horizontal tensions for mooring chains with different specific masses ($m_a$).

Figure 9 shows the shape of a mooring line, with specific mass 10 [kg/m], in *Modelica* and *Orcaflex* when the top end is placed at $X$=60 [m], and at 80 [m] with $z$= 0 [m]. When a uniform current of 1 [m/s] is applied across the full depth of the water-column, the *Orcaflex* line, based on the lumped mass model, deflects under the influence of the current. The deflection is not expected to be large enough to cause considerable difference in the fluid loading experienced by the mooring line. However, it is evident that the static catenary model would not capture the forces that result as a consequence of the dynamics of the mooring line itself.

Figure 10 shows the surge and heave response of the above free-floating buoy, when moored with a mooring line of specific mass 10 [kg/m], under different conditions of wave and current. It was noticed that the model failed to simulate when the acceleration forces due to the fluid and the motion of the chain were considered, using the **CatenaryMooring_MfCW** component model. Hence the

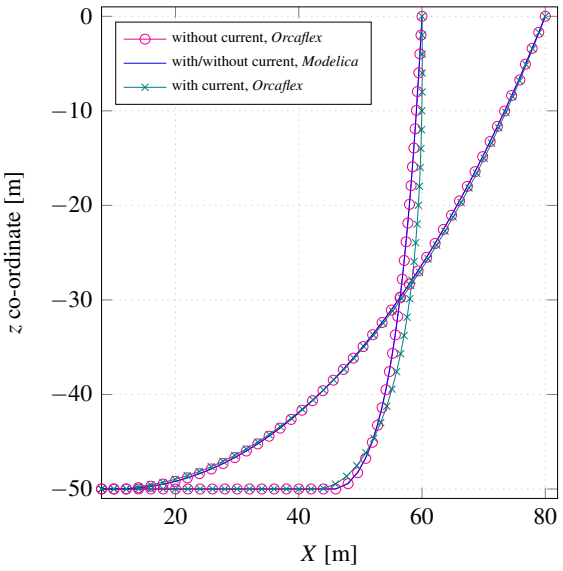


**Figure 9.** Shape of the mooring line.

results shown are with the **CatenaryMooring_MfC** component model. The combined wave-current velocity and accleration loads, and inertial loads due to the structural response of the mooring chain, are inherent in the *Orcaflex* model, while they are not accounted for by the present *Modelica* model. The phase difference in the response between the models may be because of this difference.

When the current velocity is reduced to 0.5 [m/s], **CatenaryMooring_MfCW** could be used for simulation, and the results are shown in Figure 11. However, the model is sluggish with many warnings for non-convergence. This could be due to the discontinuities in the accelerations of the segment mid-points, calculated based on the instantaneous static catenary shape. An example of the vertical component of the acceleration of the mid-point of the second segment from the top-end of the mooring, is shown in Figure 11c.

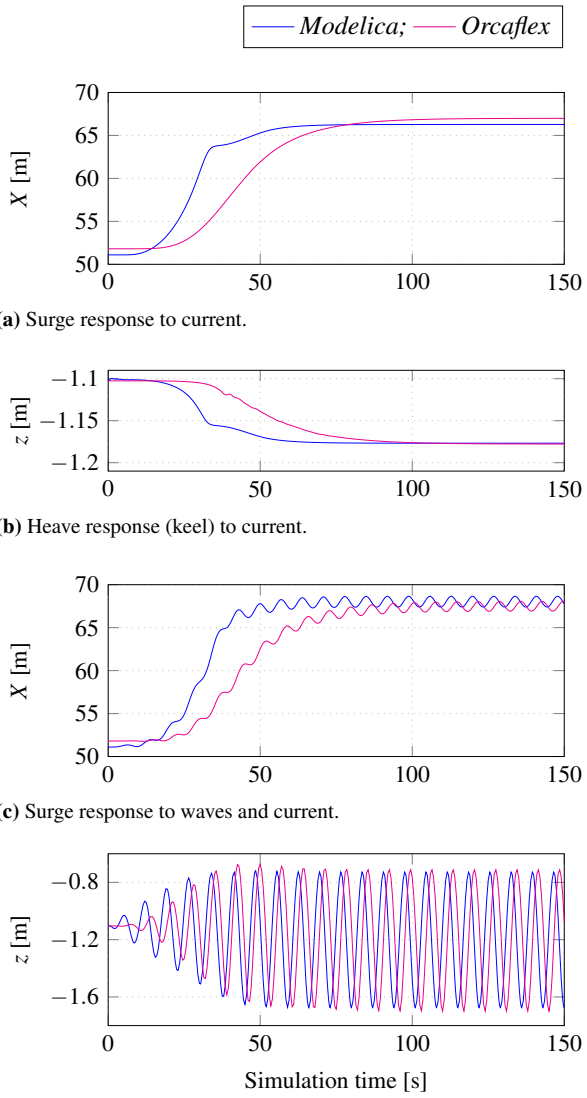


**(a)** Surge response to current.

**(b)** Heave response (keel) to current.

**(c)** Surge response to waves and current.

**(d)** Heave response (keel) to waves and current.

**Figure 10.** Hydrodynamic response of a moored cylindrical buoy.

## 5 Conclusion

Implementation of the theory to develop *Modelica* component-models for a non-diffracting cylindrical object, and for a quasi-static mooring catenary, is described in detail. Simulations to determine the hydrodynamic response of a free-floating cylinder are carried out, and the results compared with a smilar model in *Orcaflex*. It is observed that the heave responses in both cases are in satisfactory agreement. Minor differences in the surge responses are reconciled based on the comparison of Morison forces on a fixed cylinder, under various loading scenarios, and it is concluded that these differences are a result of the differences in the ramp-up functions used in this *Modelica* model and in *Orcaflex*, and hence, do not constitute *errors* in the simulation results.

The static mooring loads, based on the catenary theory in the present *Modelica* model, and those based on the lumped-mass spring-damper system of the *Orcaflex* model, are demostrated to have satisfactory agreement. The comparison between mooring configurations under different loading scenarios points out the probability that differences in the fluid loading of the mooring line, as a result of the deviation of the mooring line from the catenary shape, might not be significant, compared with the contributions from the dynamics of the mooring line itself, which the present *Modelica* model does not capture.

The simulations of a moored floating cylinder further demostrate the satisfactory agreement between this *Modelica* model and a similar *Orcaflex* model. The simulations bring out the deficiencies caused by the assumptions of the quasi-static catenary, which is not in agreement with the actual physics of the system.

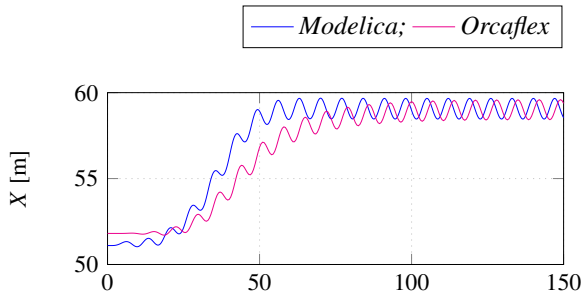


**(a)** Surge response.

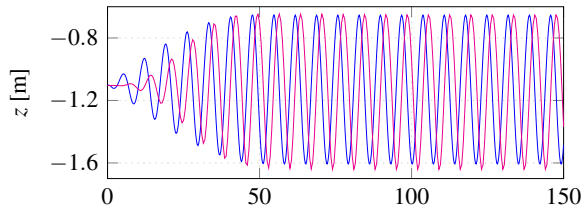


**(b)** Heave response (keel).

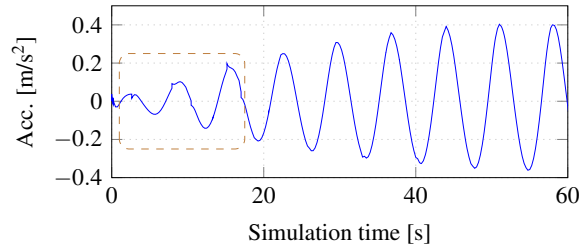


**(c)** Vertical acceleration of the second chain-link from the fairlead.

**Figure 11.** Moored cylindrical buoy in waves and reduced current.

To overcome the deficiency of not being able to account for the mooring line dynamics, and to mitigate issues as seen in Figure 11c, a *Modelica* mooring component-model based on the lumped-mass spring-damper approach is being developed, along with a frequency-domain hyrdodynamic analysis component-model, which would enable the generation of hydrodynamic parameters for diffracting objects. The initial results appear promising and will be the topic of discussion in a future work.

## 6 Acknowledgements

The research in this paper has received funding from the Research Council of Norway, SFI Offshore Mechatronics, project number 90034210.

## References

Subratha Kumar Chakrabarti. *Hydrodynamics of Offshore Structures*. Computational Mechanics Publications, and Springer-Verlag, Dorchester, Great Britain, 1987. ISBN 0-905451-66-X.

O.M. Faltinsen. *Sea Loads on Ships and Offshore Structures*. Cambridge University Press, 1999. ISBN 0-521-45870-6.

O.M. Faltinsen and F.C. Michelsen. Motion of large structures in waves at zero froude numbers. *Read at the International Symposium on the Dynamics of Marine Vehicles and Structures in Waves, London*, 1974.

MIT. *Lecture Notes on Mooring Dynamics-II*. Massachusetts Institute of Technology, 2011. URL `ocw.mit.edu/courses/mechanical-engineering/2-019-design-of-ocean-systems-spring-2011/lecture-notes/MIT2_019S11_MD2.pdf`.

J. N. Newman and C. H. Lee. Boundary-element methods in offshore structure analysis. *Journal of Offshore Mechanics and Arctic Engineering*, 124:81–89, May 2002. doi:10.1115/1.1464561.

J.N Newman. *Marine Hydrodynamics*. The MIT Press, Cambridge, Massachusetts, 1989. ISBN 0-262-14026-8.

Orcina. *Orcaflex Manual- Version 9.1a*. Orcina, 2010. URL `citeseerx.ist.psu.edu/viewdoc/download?doi=10.1.1.121.721&rep=rep1&type=pdf`.

Yan-Lin Shao and O.M. Flatinsen. A harmonic polynomial cell (hpc) method for 3d laplace equation with application in marine hydrodynamics. *Journal of Computational Physics*, (274):312–314, 2014.

SINTEF. *Handbook on Design and Operation of Flexible Pipes*. 2014. URL `sintef.no/en/latest-news/updated-handbook-on-design-and-operation-of-flexible-pipes/`.

Jeremy B. Tatum. *Lecture Notes on the Catenary*. University of Victoria, 2004. URL `astrowww.phys.uvic.ca/~tatum/classmechs/class18.pdf`.

A.H. Techet. *Lecture Notes on the Design Principles for Ocean Vehicles*. Massachusetts Institute of Technology, 2005. URL `ocw.mit.edu/courses/mechanical-engineering/2-22-design-principles-for-ocean-vehicles-13-42-spring-2005/readings/r10_froudekrylov.pdf`.

Savin Viswanathan and Christian Holden. Towards the development of an ocean engineering library for openmodelica. In *Proceedings of the ASME 2019 38th International Conference on Ocean, Offshore and Arctic Engineering.*, volume 7B: Ocean Engineering, OMAE2019-95054, June, 2019. URL `doi.org/10.1115/OMAE2019-95054`.

Savin Viswanathan and Christian Holden. Modelica component-models for oceanic surface-waves and depth varying current. *Proceedings of the American Modelica Conference*, March, 2020. The referring paper and the referred paper are part of the proceedings of the same conference.

Ronald W. Yeung. Added mass and damping of a vertical cylinder in finite-depth waters. *Applied Ocean Research*, 3(3): 119–133, 1981.